

Spin effect induced momentum spiral and asymmetry degree in pair production

Li-Na Hu,¹ Hong-Hao Fan,¹ Orkash Amat,¹ Suo Tang^{1,2}, and Bai-Song Xie^{1,3,*}

¹Key Laboratory of Beam Technology of the Ministry of Education, and School of Physics and Astronomy, Beijing Normal University, Beijing 100875, China

²College of Physics and Optoelectronic Engineering, Ocean University of China, Qingdao, Shandong 266100, China

³Institute of Radiation Technology, Beijing Academy of Science and Technology, Beijing 100875, China



(Received 27 February 2024; accepted 1 August 2024; published 10 September 2024)

Spin effect on the pair production under circularly polarized fields is investigated. Significantly different from what momentum spirals caused by two counterrotating fields with a time delay, we find for the first time that the spirals can also be induced due to the particle spin effect even if in a single field. We further examine the bichromatic combinational fields. The inhomogeneous spiral structures can be observed in the momentum spectrum; in particular, the spiral not only does exist in two cases of spin, but also is about 2 orders of magnitude amplified compared with that in the single field. Meanwhile, the spin asymmetry degree on the momentum distributions is investigated, and it was found that the effect of spin flip exists with an increased time delay between two fields. The spin asymmetry degree on the number density can reach to 98% in certain conditions. These results indicate that the signatures of created particles, especially the spiral structures, are strongly associated with information pertaining to the laser field as well as the created particle spin, which can deepen the understanding of vacuum pair production.

DOI: [10.1103/PhysRevD.110.056013](https://doi.org/10.1103/PhysRevD.110.056013)

I. INTRODUCTION

In the presence of a strong background field, the quantum electrodynamic (QED) vacuum becomes unstable and decays into electron-positron pairs [1–8]. A great deal of research has focused on the momentum distribution and number density of created pairs for different external fields. The momentum distribution exhibits a wealth of features such as effective mass signatures [9], the self-bunching effect [10], the ponderomotive force effect [11], the multiple-slit interference effect [12], and node structures [13], as well as recently discovered spiral structures [14–16].

Indeed, spiral structures have been widely investigated in many areas in past years, for example, in atomic and molecular ionization [17–22], nonlinear optics [23], type-II superconductors [24], plasmas physics [25,26], atomic condensates [27], and so on. Interestingly, recent investigations indicate that the momentum spirals have been discovered in electron-positron pair production [14–16], which are generated by two counterrotating fields with a

time delay. It should be noted that the spirals with even and odd numbers of arms are attributed to the fields by the same color [14,15] and by the different colors [16], respectively.

On the other hand, it is known that the spin effect of created particles plays a critical role in vacuum pair production [28–31]. For example, Strobel *et al.* demonstrated that the spin distribution of produced pairs is generally not 1:1 in the Schwinger pair production by the rotating electric fields depending on time [28]. Blinne *et al.* pointed out that the pair production in different spin states is unequal for a constant rotating field [29]. Interestingly, we found that, for a circularly polarized (CP) field, the number density of created bosons is the geometric mean, i.e., the square root of the spin-up number density times that of spin-down [30], and that, for arbitrarily polarized fields with several periods, the degree of spin polarization roughly increases with γ , where $\gamma = m\omega c/eE_0$ ($c = 1$) is the Keldysh adiabatic parameter and m and $-e$ denote electron mass and charge, respectively. Recently, Kohlfürst showed the power of the photon absorption model by demonstrating how to identify the imprint that the different spin states leave on the electron-positron angular distribution, and obtained the spin-dependent particle production amplitudes [31]. Moreover, spin or/and helicity resolved momentum distributions on pair production have been reported via different approaches such as scattering matrix [32] and quantum kinetic equations [33,34].

*Contact author: bsxie@bnu.edu.cn

Published by the American Physical Society under the terms of the [Creative Commons Attribution 4.0 International license](https://creativecommons.org/licenses/by/4.0/). Further distribution of this work must maintain attribution to the author(s) and the published article's title, journal citation, and DOI. Funded by SCOAP³.

To our knowledge, the previous momentum spirals are caused by the opposite photons' spin in two counterrotating fields with a time delay [14–16]. However, whether the spin of created particles can create a momentum spiral has not yet been reported. Therefore, as this is an important concern, we shall investigate the problem in this paper. The focus is on considering the spin induced momentum spiral by the single field, and the spiral structure as well as the spin asymmetry degree under the bichromatic combination fields. For the single field, it is found that there is no momentum spiral when the spin of created particles is parallel to the direction of the laser field ($s = +1$). Surprisingly, when the spin is antiparallel to the field direction ($s = -1$), there exists an obvious spiral structure in the momentum spectrum. And the spiral in the few periods field is more remarkable than that in the several periods field. On the other hand, for the bichromatic combination fields, the spiral does exist whether the spin is parallel ($s = 1$) or antiparallel ($s = -1$). Not only is the unobserved spiral in a single field seen in the two fields, but also the observed spiral in a single field is amplified about 2 orders of magnitude larger in the bichromatic fields. Meanwhile, it is found that the larger the time delay between the two fields, the more pronounced the spiral structure. Finally, by adjusting appropriate field parameters, we can also obtain a high spin asymmetry degree of created particles.

Our considered electric field form is associated with either a single field or a combination of two fields with a little different strength and frequency between them. For the single field, the form is given as

$$\mathbf{E}(t) = \mathbf{E}_1(t) = \frac{E_1}{\cosh(\frac{t}{\tau_1})} [\cos(\omega_1 t) \mathbf{e}_x + \delta_1 \sin(\omega_1 t) \mathbf{e}_y], \quad (1)$$

or

$$\begin{aligned} \mathbf{E}(t) = \mathbf{E}_2(t) = & \frac{E_2}{\cosh(\frac{t-T_d}{\tau_2})} [\cos(\omega_2(t-T_d)) \mathbf{e}_x \\ & + \delta_2 \sin(\omega_2(t-T_d)) \mathbf{e}_y]. \end{aligned} \quad (2)$$

And for the combined field case, it is given by

$$\mathbf{E}(t) = \mathbf{E}_1(t) + \mathbf{E}_2(t), \quad (3)$$

where $E_{1,2} = E_{01,02}/\sqrt{1 + \delta_{1,2}^2}$ are the field strengths ($|\delta_{1,2}| = 1$ are the CP degrees), $\omega_{1,2}$ are the field frequencies, $\tau_{1,2} = N2\pi/\omega_{1,2}$ denote the pulse duration (N determines the number of periods in the individual pulse), and $T_d = GT = G(\tau_1 + \tau_2)$ is the time delay between the two pulses, where G is a dimensionless quantity. In our study, the typical field parameters are set as $E_{01} = 0.1\sqrt{2}E_{\text{cr}}$ ($E_{\text{cr}} = m^2 c^3 / e\hbar \approx 1.3 \times 10^{16}$ V/cm denotes Schwinger

critical field strength), $E_{02} = 0.07\sqrt{2}E_{\text{cr}}$, $\delta_1 = -1$, $\delta_2 = 1$, $\omega_1 = 0.44$, $\omega_2 = 0.55$. Note that throughout this paper $\hbar = c = m = 1$ is used.

We employ the equal-time Dirac-Heisenberg-Wigner (DHW) formalism [28,29,35–38], a relativistic phase-space quantum kinetic approach, which has been widely applied to study pair production in arbitrary electromagnetic fields [10,39–46]. For the spatially homogeneous and time-dependent electric field presented in our study, the complete DHW equations of motion can be reduced to the following form [14,29,46]:

$$\begin{aligned} \dot{f} &= \frac{e\mathbf{E} \cdot \mathbf{v}}{2\Omega}, \\ \dot{\mathbf{v}} &= \frac{2}{\Omega^3} [(e\mathbf{E} \cdot \mathbf{p})\mathbf{p} - e\mathbf{E}\Omega^2](f - 1) - \frac{(e\mathbf{E} \cdot \mathbf{v})\mathbf{p}}{\Omega^2} \\ &\quad - 2\mathbf{p} \times \mathbf{a} - 2m\mathbf{t}, \\ \dot{\mathbf{a}} &= -2\mathbf{p} \times \mathbf{v}, \\ \dot{\mathbf{t}} &= \frac{2}{m} [m^2\mathbf{v} + (\mathbf{p} \cdot \mathbf{v})\mathbf{p}], \end{aligned} \quad (4)$$

with initial conditions $f(\mathbf{q}, -\infty) = 0$, $\mathbf{v}(\mathbf{q}, -\infty) = \mathbf{a}(\mathbf{q}, -\infty) = \mathbf{t}(\mathbf{q}, -\infty) = 0$, where f is the single-particle momentum distribution function, \mathbf{v} is associated with the current density \mathbf{v} , \mathbf{a} denotes spin density, and the projection of the \mathbf{t} in the direction of momentum determines the rate of change of the mass density [31,35,36]. $\Omega = \sqrt{m^2 + (\mathbf{q} - e\mathbf{A}(t))^2}$ represents the total energy of particles, \mathbf{q} is the canonical momentum related to the kinetic momentum $\mathbf{p}(t) = \mathbf{q} - e\mathbf{A}(t)$, and $\mathbf{A}(t)$ is the vector potential of the electric field $\mathbf{E}(t)$. By integrating $f(\mathbf{q}, t)$ over full momenta at $t \rightarrow +\infty$, we can obtain the number density of created particles:

$$n = \lim_{t \rightarrow +\infty} \int \frac{d^3q}{(2\pi)^3} f(\mathbf{q}, t). \quad (5)$$

Note that the above f and n are the forms without considering the spin of created particles. When considering the spin, the single-particle momentum distribution function can be changed as [29,30]

$$f_s = \frac{1}{2}(f + s\delta f_{\text{sc}}), \quad (6)$$

where $s = \pm 1$, $\delta f_{\text{sc}} = \frac{q_z}{\epsilon_\perp} \delta f_c + \frac{m}{\epsilon_\perp} \delta f_{\mu_z}$ is associated with the chiral asymmetry $\delta f_c = \frac{1}{2\Omega} \mathbf{p} \cdot \mathbf{a}$ and the magnetic moment asymmetry $\delta f_{\mu_z} = \frac{1}{2\Omega} (ma_z + (\mathbf{p} \times \mathbf{t})_z)$, $\epsilon_\perp = \sqrt{m^2 + q_z^2}$. Also the corresponding number density considering the spin could be modified as $n_s = \lim_{t \rightarrow +\infty} \int \frac{d^3q}{(2\pi)^3} f_s(\mathbf{q}, t)$.

II. MOMENTUM DISTRIBUTION

The momentum spectra of created particles in the single field $\mathbf{E}_1(t)$ and the bichromatic combination fields with $N = 0.5$ are shown in Fig. 1. It is found that under the $\mathbf{E}_1(t)$, for $f(q_x, q_y)$, there is no obvious spiral structure, but the distribution presents a good symmetry in the q_x direction; see Fig. 1(a). The symmetry is related to the fact that the electric field in the x direction is an even function [13,15]. Meanwhile, one can see that $f(q_x, q_y)$ is mainly distributed in the lower half plane, where it dominates the contribution to the pair production, which is consistent with the results in terms of the turning points by $\Omega(\mathbf{q}, t) = 0$ [47,48]. For $f_{\pm}(q_x, q_y)$, however, the momentum distributions present a clear difference. We find that the $f_+(q_x, q_y)$ shown in Fig. 1(b) is dominant. But surprisingly, there exists a remarkable spiral structure in $f_-(q_x, q_y)$ [see Fig. 1(c)], although it is about 2 orders of magnitude weaker than $f_+(q_x, q_y)$. Actually, we have done

the results of $\mathbf{E}_2(t)$ (patterns are not shown), which are similar to the results of $\mathbf{E}_1(t)$, except that the momentum distribution shifts from the lower half plane to the upper half plane, and the spiral structures appear in $f_+(q_x, q_y)$. These are not surprising since the spin directions of the fields $\mathbf{E}_1(t)$ and $\mathbf{E}_2(t)$ are opposite to each other.

Note that when we consider the spin of created particles, there are two ways for spin alignment in a pair of spin-1/2 particles: parallel and antiparallel [31]. Since the propagation direction of our field [Eq. (1)] is along the z axis, for the parallel whereby the spin directions of the electrons and positrons are parallel to the field direction, the total spin is $S = 1/2 + 1/2 = 1$, while for the antiparallel whereby the direction of one of the particles is antiparallel to the field direction, the total spin is $S = 0$. Obviously, it is found that the distribution of created pairs for $S = 1$ is larger than that for $S = 0$, as shown in Figs. 1(b) and 1(c), respectively, which results in agreement with that in Ref. [31].

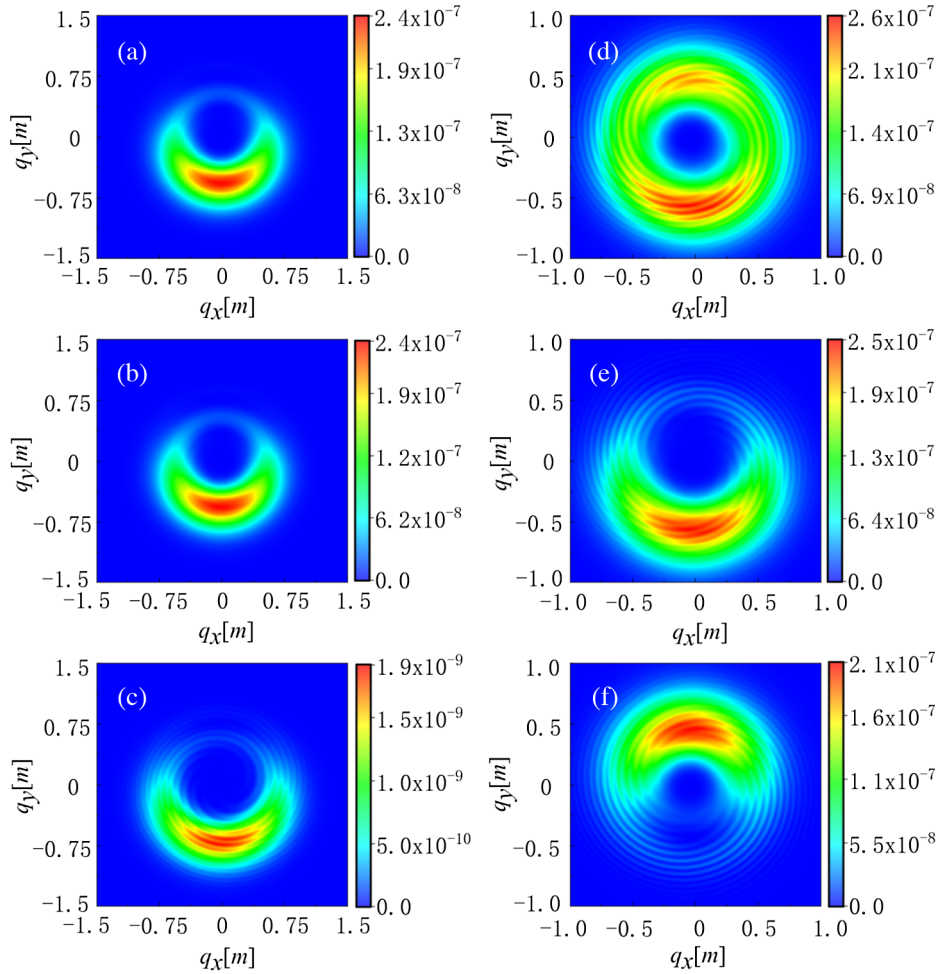


FIG. 1. Momentum spectra of created particles in the (q_x, q_y) plane [where $q_z = 0$] under the single field $\mathbf{E}_1(t)$ (for (a)–(c)) and the bichromatic combination fields for $T_d = 8T$ [for (d)–(f)] with $N = 0.5$. From top to bottom, each row (a) and (d), (b) and (e), (c) and (f) corresponds to $f(q_x, q_y)$, $f_+(q_x, q_y)$, and $f_-(q_x, q_y)$ [refer to Eq. (6)], respectively. Other parameters are $E_{01} = 0.1\sqrt{2}E_{cr}$, $\delta_1 = -1$, $\omega_1 = 0.44$, $E_{02} = 0.07\sqrt{2}E_{cr}$, $\delta_2 = 1$, $\omega_2 = 0.55$.

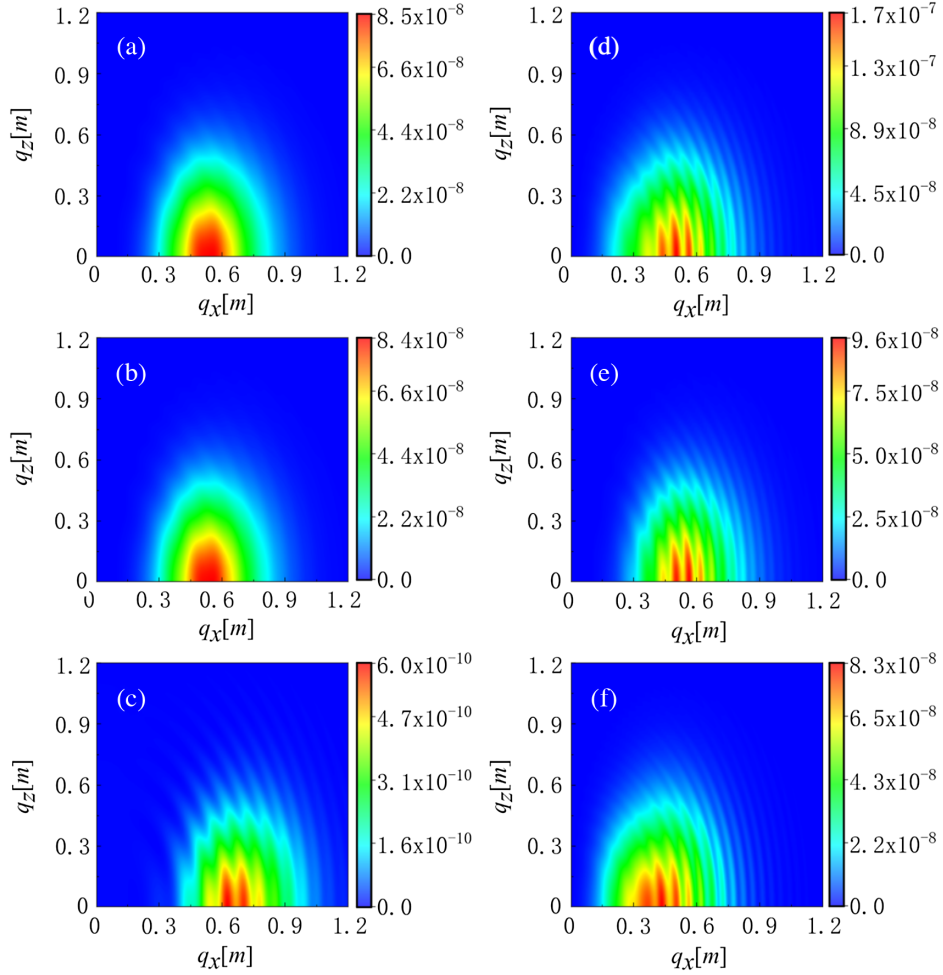


FIG. 2. The same as in Fig. 1 except that the distributions are in the (q_x, q_z) plane (where $q_y = 0$).

It should be emphasized that the momentum spirals in a single field in our study mentioned above are induced by the spin effect of created particles, which is different from the previous findings [14–16] that are caused by the opposite photons' spin in two counterrotating fields with a time delay.

Under the bichromatic combination fields with $T_d = 8T$, it is found that there is a remarkable spiral pattern in the momentum spectra. For $f(q_x, q_y)$, the spiral structure is constituted of nine arms, and its distribution in the whole plane is nonuniform with more strength in the lower half plane; see Fig. 1(d). This phenomenon can be understood in connection with the results of a single field. It is known that the momentum spectra $f(q_x, q_y)$ of $\mathbf{E}_1(t)$ and $\mathbf{E}_2(t)$ are mainly distributed in the lower half plane and the upper half plane, respectively. And since the field strength of $\mathbf{E}_1(t)$ is larger than that of $\mathbf{E}_2(t)$, the $f(q_x, q_y)$ for $\mathbf{E}_1(t)$ is stronger than that for $\mathbf{E}_2(t)$. When the time delay is large, the two fields $\mathbf{E}_1(t)$ and $\mathbf{E}_2(t)$ are almost independent, which leads to the result under the combined fields being almost a superposition of the ones under the two individual fields.

Therefore, for $T_d = 8T$, the $f(q_x, q_y)$ of the lower half plane is stronger than that of the upper half plane.

For $f_{\pm}(q_x, q_y)$, one can see that the spiral of $f_+(q_x, q_y)$ is mainly distributed in the lower half plane, as shown in Fig. 1(e), while the result of $f_-(q_x, q_y)$ is opposite; see Fig. 1(f). The results are also associated with the momentum distributions in a single field. Specifically, let us first understand the result of $f_+(q_x, q_y)$ in Fig. 1(e). In the combined fields with a larger time delay, we can think that $f_+(q_x, q_y)$ consists of the $f_+(q_x, q_y)$ of $\mathbf{E}_1(t)$ and $\mathbf{E}_2(t)$. It is known that the $f_+(q_x, q_y)$ of $\mathbf{E}_1(t)$ and $\mathbf{E}_2(t)$ are predominantly distributed in the lower half plane and the upper half plane, respectively, and there exists an obvious spiral structure in the $f_+(q_x, q_y)$ of $\mathbf{E}_2(t)$. Meanwhile, the $f_+(q_x, q_y)$ of $\mathbf{E}_1(t)$ is about 2 orders of magnitude larger than that of $\mathbf{E}_2(t)$. When the $\mathbf{E}_1(t)$ and $\mathbf{E}_2(t)$ are combined, there should be $f_+(q_x, q_y)$ in the whole plane. But the $f_+(q_x, q_y)$ of $\mathbf{E}_1(t)$ mainly contributes to the position of distribution, while $f_+(q_x, q_y)$ of $\mathbf{E}_2(t)$ mainly contributes to the spiral structure. Therefore, these results ultimately lead to $f_+(q_x, q_y)$ in the combined fields mainly distributed

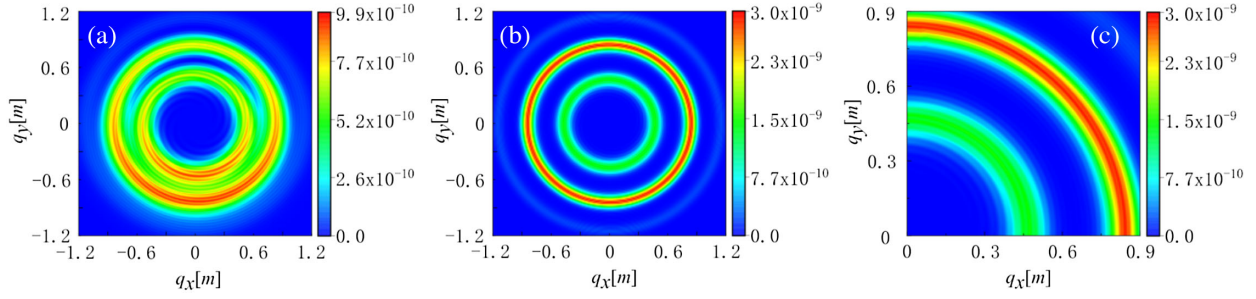


FIG. 3. Momentum spectra $f_-(q_x, q_y)$ of created particles in the (q_x, q_y) plane (where $q_z = 0$) for the single field $\mathbf{E}_1(t)$ with different N . (a) and (b) correspond to $N = 1$ and $N = 2$, respectively. (c) is the amplified result of (b).

in the lower half plane and accompanied by a remarkable spiral structure, where the spiral is about 2 orders of magnitude greater than that in the single field. For the results of $f_-(q_x, q_y)$ in the combined fields, a similar understanding can be performed.

Now let us see the momentum distributions in the (q_x, q_z) plane (where $q_y = 0$) under the single or/and the bichromatic combined fields with $N = 0.5$; the results are shown in Fig. 2. Owing to the distributions being symmetric about both $q_x = 0$ and $q_z = 0$, we only show a quarter of the results here. Compared to the results in the previous work [29] for the single field, our $f_-(q_x, q_z)$ is similar to that f_+ of Fig. 5 in [29] since the field is opposite to ours so that our f_- corresponds to their f_+ . However, our $f(q_x, q_z)$ and $f_+(q_x, q_z)$ are different from them. We think the differences may be attributed to the field of [29] being for the several periods case, whereas ours is for the few periods case. In [29] they emphasized that the pattern is a typical interference effect; however, in our case here we have observed a delicate relation of interference to the weak spiral. For the combination fields, see the right column of Fig. 2; similar to the results in the (q_x, q_y) plane of Fig. 1, all momentum distributions have exhibited the interference or/and weak spiral including the magnitude amplifier effect [Fig. 2(f)] compared to that in the single field [Fig. 2(c)].

It is noted that the authors of Ref. [33] recently proposed another approach to get the momentum distribution taking into account the spin effect of created particles. We have also computed the above results using this method; compared with our results, we find that when $q_z = 0$, Fig. 1 obtained by the two methods is completely consistent. When $q_z \neq 0$, Fig. 2 obtained by the two methods is slightly different (maximum difference is within 37%): the patterns and orders of magnitude are almost the same, and only the distribution ranges are slightly different, which does not affect the final results and conclusions.

As N increases from $N = 0.5$ to $N = 1$ and $N = 2$, we take the results of $f_-(q_x, q_y)$ in the $\mathbf{E}_1(t)$ as an example (see Fig. 3), and find that the distribution range of the spiral becomes larger and the spiral arms become thinner as well as longer, while the symmetry of the spiral becomes better in both the q_x and q_y directions [To see more clearly, we

amplify the result of $N = 2$ and show only the quarter (upper right corner) of the result in Fig. 2(b), as shown in Fig. 3(c)]. These phenomena are associated with the fact that the pair production tends more and more to be the multiphoton absorption process with increasing N .

III. SPIN ASYMMETRY DEGREE

For convenience, the spin asymmetry degree on the momentum distributions $f(q_x, q_y)$ was defined as

$$\kappa_f = \frac{f_+(q_x, q_y) - f_-(q_x, q_y)}{f_+(q_x, q_y) + f_-(q_x, q_y)}. \quad (7)$$

Figure 4 shows the spin asymmetry degree κ_f in the combined fields with different time delays, in which there are the following three cases in general. (i) For $T_d = 0$, $f_+(q_x, q_y)$ and $f_-(q_x, q_y)$ are uniformly inter-nested in the whole plane, and the fraction of two distributions is almost 1:1. (ii) For the small time delay $T_d = T$, there is a preliminary separation between $f_+(q_x, q_y)$ and $f_-(q_x, q_y)$, but $f_-(q_x, q_y)$ is dominant. (iii) For the large time delay $T_d = 8T$, $f_+(q_x, q_y)$ and $f_-(q_x, q_y)$ are completely separated, in which the upper half plane and the lower half plane are dominated by $f_-(q_x, q_y)$ and $f_+(q_x, q_y)$, respectively.

First, for $T_d = 0$, one can see that the distribution of κ_f has a good symmetry in the q_x direction [see Fig. 4(a)], which is related to the symmetry of corresponding momentum distributions. Moreover, it is found that $f_+(q_x, q_y)$ and $f_-(q_x, q_y)$ are uniformly inter-nested in Fig. 4(a). This is because the fraction of $f_+(q_x, q_y)$ and $f_-(q_x, q_y)$ is almost 1:1. Second, as the time delay increases to $T_d = T$, the symmetry of κ_f is destroyed; at the same time, a wide and nonuniform spiral structure can be observed [see Fig. 4(b)]. In addition, there is a preliminary separation between $f_+(q_x, q_y)$ and $f_-(q_x, q_y)$, where the lower half plane is mainly dominated by $f_+(q_x, q_y)$, while the results in the upper half plane are opposite. However, in the entire plane, $f_-(q_x, q_y)$ is dominant.

Third, as T_d further increases to $T_d = 8T$, the distribution of κ_f is approximately symmetric in the

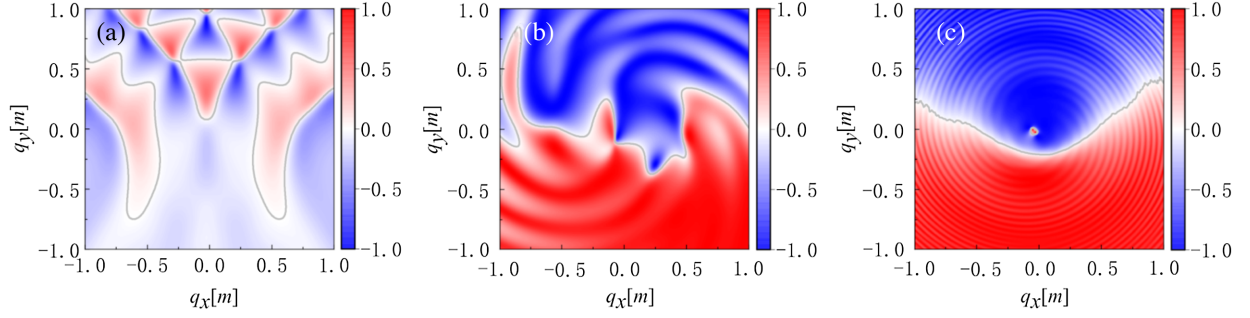


FIG. 4. Spin asymmetry degree on the momentum spectra in the (q_x, q_y) plane (where $q_z = 0$) under the combination fields for different time delays with $N = 0.5$. (a), (b) and (c) correspond to $T_d = 0$, $T_d = T$, and $T_d = 8T$, respectively. The gray line denotes $\kappa_f = 0$.

q_x direction, and we can observe the thin and uniform spiral fringes; see Fig. 4(c). Moreover, it is found that there exists a clear dividing line in this distribution, where the lower half plane and the upper half plane are primarily dominated by $f_+(q_x, q_y)$ and $f_-(q_x, q_y)$, respectively, which are associated with the ones of Figs. 1(e) and 1(f). This clear dividing phenomenon may be attributed to the fact that when $\mathbf{E}_1(t)$ and $\mathbf{E}_2(t)$ are combined, as we described above, the result with a large time delay is almost caused by the superposition of the results in two individual fields.

The spin asymmetry degree on the number density of created particles in the combined fields with different time delays is shown in Fig. 5, where we define the spin asymmetry degree as $\kappa_n = \kappa_n^1 - \kappa_n^2$ with $\kappa_n^1 = n_+ / (n_+ + n_-)$ and $\kappa_n^2 = n_- / (n_+ + n_-)$. From Fig. 5(a), we find that for $T_d = 0$, κ_n^1 is smaller than κ_n^2 , i.e., the n_- is dominant.

As T_d increases, a crossing point between κ_n^1 and κ_n^2 occurs, which is located in the range of $T_d = 1 \sim 2T$. It indicates that there exists a spin-flip effect in this range. When $T_d \geq 2T$, κ_n^1 is larger than κ_n^2 , i.e., n_+ is dominant. Based on the above results, we can expect to control the momentum spectrum by changing the time delay; for example, if we want to obtain a momentum spectrum dominated by $f_-(q_x, q_y)$, we can set the time delay T_d to be smaller, and if we want to get the spectrum dominated by $f_+(q_x, q_y)$, the T_d needs to be extended. Moreover, one can see that with the increase of T_d , the κ_n first increases and then remains unchanged as 12%. In order to obtain a higher spin asymmetry degree, we have performed some other simulations, for example the result shown in Fig. 5(b). It is found that κ_n monotonically decreases with increasing T_d ; specifically, it decreases from -50% at $T_d = 0$ and eventually reaches -98% at $T_d = 8T$.

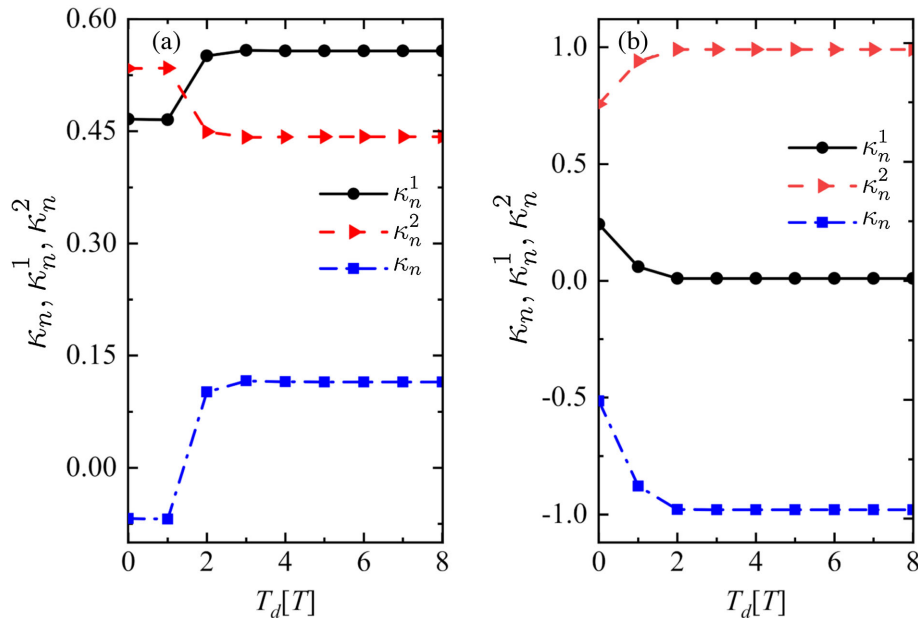


FIG. 5. Spin asymmetry degree on the number density of created particle dependence on time delays by the combinational fields. (a) for $N = 0.5$. (b) for $N = 2$, $E_{02} = 0.05\sqrt{2}E_{cr}$, and $\omega_2 = 1.2$. Other parameters are the same as in Fig. 1.

IV. DISCUSSION

Different from the previous studies [14,15], we found that the spin can induce the momentum spirals in a single field. The bichromatic combined fields lead to an inhomogeneous spiral structures of the momentum, especially, the spiral pattern does exist in both f_+ and f_- , and it is about 2 orders of magnitude larger than the single field. It seems that one field creates spiral “seed” for a certain spin type, while the other field plays a role as the “amplifier” to this spiral. For the opposite spin case, the roles of “seed” and “amplifier” played by the fields are exchangeable.

It is known that the purely time-dependent electric field actually consists of two counter-propagating waves [49], and they are focused on the narrow regime of original electron Compton scales, i.e., a dipole approximation is met. For our single field, it is equivalent to a combination of a left-handed wave and a right-handed wave, and the two counterpropagating waves are attributing for most of the interaction time at the focusing spatial scale. So this is very similar to the case of combined fields that consist of two counterrotating pulses. This is maybe a reason why the spiral can exist even if the single field is present.

These results suggest that the spin effect of created particles plays an important role in momentum spiral on

pair production. It not only can induce the momentum spiral in a single field, but can also contribute to the formation of the spiral in the bichromatic combinational fields as well as the appearance of the spin-flip effect. Moreover, the momentum spiral due to the spin is sensitive to the field parameters. It is found that either the larger the time delay or the smaller the number of periods, the more pronounced the momentum spiral, which provides a flexible way to control the spiral features. While we have only considered the simple case of CP fields, we speculate that more delicate spin effects exist in different cases of fields, and further features associated with the momentum patterns on pair production are expected.

ACKNOWLEDGMENTS

We are grateful to Z. L. Li and C. Kohlfürst for helpful discussions. We are thankful to the anonymous referee for helpful suggestions to improve the manuscript. This work was supported by the National Natural Science Foundation of China (NSFC) under Grants No. 12375240, No. 11935008, and No. 12104428. The computation was carried out at the HSCC of the Beijing Normal University.

-
- [1] F. Sauter, Über das Verhalten eines Elektrons im homogenen elektrischen Feld nach der relativistischen Theorie Diracs, *Z. Phys.* **69**, 742 (1931).
 - [2] W. Heisenberg and H. Euler, Consequences of Dirac’s theory of the positron, *Z. Phys.* **98**, 714 (1936).
 - [3] A. Di Piazza, C. Müller, K. Z. Hatsagortsyan, and C. H. Keitel, Extremely high-intensity laser interactions with fundamental quantum systems, *Rev. Mod. Phys.* **84**, 1177 (2012).
 - [4] A. Fedotov, A. Ilderton, F. Karbstein, B. King, D. Seipt, H. Taya, and G. Torgrimsson, Advances in QED with intense background fields, *Phys. Rep.* **1010**, 1 (2023).
 - [5] B. S. Xie, Z. L. Li, and S. Tang, Electron-positron pair production in ultrastrong laser fields, *Matter Radiation. Extremes* **2**, 225 (2017).
 - [6] G. V. Dunne, New strong-field QED effects at ELI: Non-perturbative vacuum pair production, *Eur. Phys. J. D* **55**, 327 (2009).
 - [7] J. S. Schwinger, On gauge invariance and vacuum polarization, *Phys. Rev.* **82**, 664 (1951).
 - [8] D. L. Burke, R. C. Field, G. Horton-Smith, J. E. Spencer, D. Walz, S. C. Berridge, W. M. Bugg, K. Shmakov, A. W. Weidemann, C. Bula, K. T. McDonald, and E. J. Prebys, Positron production in multi-photon light by light scattering, *Phys. Rev. Lett.* **79**, 1626 (1997); C. Bamber *et al.*, Studies of nonlinear QED in collisions of 46.6-GeV electrons with intense laser pulses, *Phys. Rev. D* **60**, 092004 (1999).
 - [9] C. Kohlfürst, H. Gies, and R. Alkofer, Effective mass signatures in multiphoton pair production, *Phys. Rev. Lett.* **112**, 050402 (2014).
 - [10] F. Hebenstreit, R. Alkofer, and H. Gies, Particle self-bunching in the Schwinger effect in spacetime-dependent electric fields, *Phys. Rev. Lett.* **107**, 180403 (2011).
 - [11] C. Kohlfürst and R. Alkofer, Ponderomotive effects in multiphoton pair production, *Phys. Rev. D* **97**, 036026 (2018).
 - [12] Z. L. Li, D. Lu, B. S. Xie, L. B. Fu, J. Liu, and B. F. Shen, Enhanced pair production in strong fields by multiple-slit interference effect with dynamically assisted Schwinger mechanism, *Phys. Rev. D* **89**, 093011 (2014).
 - [13] Z. L. Li, D. Lu, B. S. Xie, B. F. Shen, L. B. Fu, and J. Liu, Nonperturbative signatures in pair production for general elliptic polarization fields, *Europhys. Lett.* **110**, 51001 (2015).
 - [14] Z. L. Li, Y. J. Li, and B. S. Xie, Momentum vortices on pairs production by two counter-rotating fields, *Phys. Rev. D* **96**, 076010 (2017).
 - [15] L. N. Hu, O. Amat, L. Wang, A. Sawut, H. H. Fan, and B. S. Xie, Momentum spirals in multiphoton pair production revisited, *Phys. Rev. D* **107**, 116010 (2023).
 - [16] Z. L. Li, B. S. Xie, and Y. J. Li, Vortices in multiphoton pair production by two-color rotating laser fields, *J. Phys. B* **52**, 025601 (2019).

- [17] J. M. Ngoko Djiokap, S. X. Hu, L. B. Madsen, N. L. Manakov, A. V. Meremianin, and Anthony F. Starace, Electron vortices in photoionization by circularly polarized attosecond pulses, *Phys. Rev. Lett.* **115**, 113004 (2015).
- [18] D. Pengel, S. Kerbstadt, D. Johannmeyer, L. Englert, T. Bayer, and M. Wollenhaupt, Electron vortices in femto-second multiphoton ionization, *Phys. Rev. Lett.* **118**, 053003 (2017).
- [19] M. M. Majczak, F. Cajiao Vélez, J. Z. Kamiński, and K. Krajewska, Carrier-envelope-phase and helicity control of electron vortices and spirals in photodetachment, *Opt. Express* **30**, 43330 (2022).
- [20] J. H. Macek, J. B. Sternberg, S. Y. Ovchinnikov, T. G Lee, and D. R. Schultz, Origin, evolution, and imaging of vortices in atomic processes, *Phys. Rev. Lett.* **102**, 143201 (2009).
- [21] K. J. Yuan, S. Chelkowski, and A. D. Bandrauk, Photoelectron momentum distributions of molecules in bichromatic circularly polarized attosecond UV laser fields, *Phys. Rev. A* **93**, 053425 (2016).
- [22] L. Geng, F. C. Vélez, J. Z. Kamiński, L. Y. Peng, and K. Krajewska, Vortex structures in photodetachment by few-cycle circularly polarized pulses, *Phys. Rev. A* **102**, 043117 (2020).
- [23] M. Harris, C. A. Hill, and J. M. Vaughan, Optical helices and spiral interference fringes, *Opt. Commun.* **106**, 161 (1994).
- [24] G. Blatter, M. V. Feigelman, V. B. Geshkenbein, A. I. Larkin, and V. M. Vinokur, Vortices in high-temperature superconductors, *Rev. Mod. Phys.* **66**, 1125 (1994).
- [25] L. Uby, M. B. Isichenko, and V. V. Yankov, Vortex filament dynamics in plasmas and superconductors, *Phys. Rev. E* **52**, 932 (1995).
- [26] P. K. Shukla and B. Eliasson, Colloquium: Fundamentals of dust-plasma interactions, *Rev. Mod. Phys.* **81**, 25 (2009).
- [27] K. W. Madison, F. Chevy, W. Wohlleben, and J. Dalibard, Vortex formation in a stirred Bose-Einstein condensate, *Phys. Rev. Lett.* **84**, 806 (2000).
- [28] E. Strobel and S. S. Xue, Semiclassical pair production rate for rotating electric fields, *Phys. Rev. D* **91**, 045016 (2015).
- [29] A. Blinne and E. Strobel, Comparison of semiclassical and Wigner function methods in pair production in rotating fields, *Phys. Rev. D* **93**, 025014 (2016).
- [30] Z. L. Li, B. S. Xie, and Y. J. Li, Boson pair production in arbitrarily polarized electric fields, *Phys. Rev. D* **100**, 076018 (2019).
- [31] C. Kohlfürst, Spin states in multiphoton pair production for circularly polarized light, *Phys. Rev. D* **99**, 096017 (2019).
- [32] M. M. Majczak, K. Krajewska, J. Z. Kaminski, and A. Bechler, Scattering matrix approach to dynamical Sauter-Schwinger process: Spin- and helicity-resolved momentum distributions, [arXiv:2403.15206](https://arxiv.org/abs/2403.15206).
- [33] I. A. Aleksandrov, A. Kudlis, and A. I. Klochai, Kinetic theory of vacuum pair production in uniform electric fields revisited, [arXiv:2403.17204](https://arxiv.org/abs/2403.17204).
- [34] I. A. Aleksandrov and A. Kudlis, Pair production in rotating electric fields via quantum kinetic equations: Resolving helicity states, *Phys. Rev. D* **110**, L011901 (2024).
- [35] C. Kohlfürst, Electron-positron pair production in inhomogeneous electromagnetic fields, Ph.D. thesis, University of Graz, 2015, [arXiv:1512.06082](https://arxiv.org/abs/1512.06082).
- [36] F. Hebenstreit, Schwinger effect in inhomogeneous electric fields, Ph.D. thesis, University of Graz, 2011, [arXiv:1106.5965](https://arxiv.org/abs/1106.5965).
- [37] I. Bialynicki-Birula, P. Gornicki, and J. Rafelski, Phase space structure of the Dirac vacuum, *Phys. Rev. D* **44**, 1825 (1991).
- [38] F. Hebenstreit, R. Alkofer, and H. Gies, Schwinger pair production in space and time-dependent electric fields: Relating the Wigner formalism to quantum kinetic theory, *Phys. Rev. D* **82**, 105026 (2010).
- [39] M. Ababekri, B. S. Xie, and J. Zhang, Effects of finite spatial extent on Schwinger pair production, *Phys. Rev. D* **100**, 016003 (2019).
- [40] C. Kohlfürst, Effect of time-dependent inhomogeneous magnetic fields on the particle momentum spectrum in electron-positron pair production, *Phys. Rev. D* **101**, 096003 (2020).
- [41] A. Blinne and H. Gies, Pair production in rotating electric fields, *Phys. Rev. D* **89**, 085001 (2014).
- [42] L. J. Li, M. Mohamedsedik, and B. S. Xie, Enhanced dynamically assisted pair production in spatial inhomogeneous electric fields with the frequency chirping, *Phys. Rev. D* **104**, 036015 (2021).
- [43] O. Olugh, Z. L. Li, B. S. Xie, and R. Alkofer, Pair production in differently polarized electric fields with frequency chirps, *Phys. Rev. D* **99**, 036003 (2019).
- [44] Z. L. Li, D. Lu, and B. S. Xie, Effects of electric field polarizations on pair production, *Phys. Rev. D* **92**, 085001 (2015).
- [45] C. Kohlfürst, Phase-space analysis of the Schwinger effect in inhomogeneous electromagnetic fields, *Eur. Phys. J. Plus* **133**, 191 (2018).
- [46] O. Olugh, Z. L. Li, and B. S. Xie, Dynamically assisted pair production for various polarizations, *Phys. Lett. B* **802**, 135259 (2020).
- [47] C. K. Dumlu and G. V. Dunne, The Stokes phenomenon and Schwinger vacuum pair production in time-dependent laser pulses, *Phys. Rev. Lett.* **104**, 250402 (2010).
- [48] J. Oertel and R. Schützhold, WKB approach to pair creation in spacetime-dependent fields: The case of a spacetime-dependent mass, *Phys. Rev. D* **99**, 125014 (2019).
- [49] C. Kohlfürst, Pair production in circularly polarized waves, [arXiv:2212.03180](https://arxiv.org/abs/2212.03180).